DOI: 10.1016/j.jcis.2013xxxxx

Sulfonated macro-RAFT agents for the surfactant-free synthesis of cerium oxide-based hybrid latexes

Jérôme Garnier[b], Jérôme Warnant[b], Patrick Lacroix-Desmazes[b,*], Pierre-Emmanuel Dufils[c], Jérôme Vinas[d] and Alex van Herk[a,*]

[a] *Institute of Chemical and Engineering Sciences, 1 Pesek Road, 627833 Singapore and Polymer Reaction Engineering group, Eindhoven University of Technology, P.O. Box 513, 5600 MB Eindhoven, The Netherlands.*
[b] *Institut Charles Gerhardt (ICG), UMR5253 CNRS/UM2/ENSCM/UM1, Ingénierie et Architectures Macromoléculaires (IAM), Ecole Nationale Supérieure de Chimie de Montpellier, 8 rue de l'Ecole Normale, 34296 Montpellier Cedex 5, France.*
[c] *High Barrier Polymers – Solvay Specialty Polymers – Avenue de la République, 39500 Tavaux, France.*
[d] *High Barrier Polymers – Solvay Specialty Polymers – Solvay Campus – Rue de Ransbeek 310, B-1120 Brussels, Belgium.*

* Corresponding authors:
Fax: +31 40 246 3966; E-mail address: A.M.v.Herk@tue.nl (A.M. van Herk)
Fax: +33 467 14 72 20; E-mail address: patrick.lacroix-desmazes@enscm.fr (P. Lacroix-Desmazes)

Abstract

Three types of amphiphatic macro-RAFT agents were employed as compatibilizers to promote the polymerization reaction at the surface of nanoceria for the synthesis of CeO_2-based hybrid latexes. Macro-RAFT copolymers and terpolymers were first synthesized employing various combinations of butyl acrylate as a hydrophobic monomer and acrylic acid (AA) and/or 2-acrylamido-2-methylpropane sulfonic acid (AMPS) as hydrophilic monomers. After characterizing the adsorption of these macro-RAFT agents at the cerium oxide surface by UV-visible spectrometry, emulsion copolymerization reactions of styrene and methyl acrylate were then carried out in the presence of the surface-modified nanoceria. Dynamic Light Scattering and cryo-Transmission Electron Microscopy were employed to confirm the hybrid structure of the final CeO_2/polymer latexes, and proved that the presence of acrylic acid units in amphiphatic macro-RAFT agents enabled an efficient formation of hybrid structures, while the presence of AMPS units, when combined with AA units, resulted in a better distribution of cerium oxide nanoclusters between latex particles.

Keywords: Emulsion polymerization; cerium oxide; hybrid latex; RAFT polymerization.

---

1. Introduction

The art of incorporating inorganic particles inside a polymer matrix, and more particularly into a polymer latex, has attracted much interest[1,2], since these mineral objects may provide improved or additional properties to the resulting hybrid material, such as, among others, enhanced mechanical properties, scratch resistance, magnetic properties, UV absorption, as well as opacity or color when employed as pigments.

Cerium oxide is a highly interesting and versatile material, owing to its multiple properties and applications as engine exhaust catalysts[3,4], polishing agents[5], solid electrolytes in fuel cells[6] or in oxygen sensors[7]. More specifically, in its nanoparticle form, CeO_2 is a very promising candidate as UV stabilizer in polymeric materials owing to its UV-filtering properties[8-10]. Nevertheless, the synthesis of inorganic/organic hybrid latexes is not straightforward, given that polymerization processes are rarely favored at the surface of inorganic particles and, therefore, often requires a preliminary step of modification of the mineral particles surface. Among the great variety of techniques designed during the past decades to improve the incorporation of inorganic particles in polymer latexes via emulsion polymerization processes[1,2,11], Nguyen et al.[12] developed an efficient and versatile strategy that strongly promotes the polymerization reaction at the surface of mineral particles: these authors employed amphiphatic macro-RAFT agents containing a random distribution of acrylic acid and *n*-butyl acrylate units to encapsulate alumina- and zirconia-coated titanium dioxide (TiO_2) and phtalocyanine blue. This technique was later extended to the synthesis of

TiO_2/polymer hybrid nanorattles[13] and to the polymer encapsulation of gibbsite[14] and lead sulfide quantum dots[15].

In a recent article[16], we successfully applied this approach to the efficient incorporation of cerium oxide nanoclusters into polymer latexes via a surfactant-free emulsion polymerization reaction, employing a neutral CeO_2 dispersion as starting material. On the one hand, we assumed that the presence of citrate molecules at the cerium oxide surface accounted for the partial engulfment of the inorganic particles by the polymer phase. On the other hand, the presence of more than one CeO_2 nanocluster per latex particle was attributed to the poor colloidal stability of hybrid particle precursors, leading to the formation of larger particles decorated with several cerium oxide nanoparticles. In the meantime, Zgheib et al.[17] reported the complete encapsulation of cerium oxide starting from a different type of nanoceria dispersion. However, due to the limited stability of this sol, confined to a narrow range of acidic pH, the adsorption of poly(BA-*co*-AA) RAFT copolymers at the surface of cerium oxide nanoparticles provoked their precipitation and prevented a complete redispersion at higher pH. As a result, the final hybrid latexes contained large aggregates of cerium oxide and monomer conversions only up to 70% could be achieved. Hence, both approaches revealed that colloidal stability remained a key factor during the synthesis of nanoceria-based hybrid latexes via the macro-RAFT agent route. Following a very different strategy, Aguirre et al.[18] reported the complete encapsulation of cerium oxide with a homogeneous distribution and a more limited aggregation of the initial CeO_2 nanoparticles. In this paper we have chosen again for the regular (surfactant free) emulsion polymerization process which has several advantages over the miniemulsion process employed in their case, where the use of an energy-consuming high shear device and the presence of extra additives in the system, such as a hydrophobic costabilizer and a conventional surfactant, is needed[18].

In this paper we propose to extend the macro-RAFT agent strategy for the emulsifier-free synthesis of cerium oxide-based polymer latexes to the use of alternative classes of amphiphatic RAFT copolymers and terpolymers bearing sulfonic acid groups. Such functions, employed in their deprotonated form in aqueous solutions, could indeed improve the colloidal stability of cerium oxide/polymer hybrid precursors and result in a better distribution of CeO_2 nanoclusters between latex particles without the addition of any conventional surfactant to the system. Furthermore, the presence of sulfonic acid groups in the macro-RAFT agent chains could enhance their solubility in water and help circumventing some practical issues encountered during the preparation of aqueous solutions of poly(BA-*co*-AA) copolymers with high butyl acrylate contents[12]. It should be mentioned that the use of an amphiphatic sulfonated macro-RAFT agent, based on butyl acrylate, acrylic acid and sodium styrene sulfonate, was already reported for the encapsulation of titanium dioxide in view to enhance the latex stability at low pH[13]. However, only few details were given about the characterization of the terpolymer, while results of its adsorption at the titanium dioxide surface were missing. Herein, the synthesis and characterization of the copolymers and terpolymers will be extensively discussed and their adsorption on the CeO_2 surface will be investigated by UV analysis. Then, the seeded emulsion polymerization will be performed for the production of CeO_2/polymer hybrid latexes.

2. Experimental

2.1. Materials

Butyl acrylate (BA, Aldrich, ≥99%) and acrylic acid (AA, Aldrich, 99%) were purified through inhibitor removing columns. 2-Acrylamido-2-methyl propane sulfonic acid

(AMPS, Aldrich, 99%) was used as received. 2,2'-Azobis(2-methylpropionitrile) (AIBN, Aldrich, 98%) was purified by recrystallization in methanol. Sodium sulfide (Aldrich, hydrate form, 30wt%), carbon disulfide (Fluka 99%), tetrabutylammonium bromide (Aldrich, 99%), benzyl chloride (Aldrich, 99%), ethanol (Biosolve), methanol (Biosolve), 1,4-dioxane (Merck), dimethyl sulfoxide (DMSO, Carlo Erba), tetrahydrofuran (THF stabilized with butylated hydroxytoluene, Biosolve) and acetic acid (Sigma-Aldrich, >99%) were used as received. Styrene (Sty, Aldrich, ≥99%) and methyl acrylate (MA, Aldrich, 99%) were purified through inhibitor removing columns. 2,2'-Azobis[N-(2-carboxyethyl)-2-methylpropionamidine] hydrate (VA-057, Wako) was used as received. Water was deionized through an ion-exchange resin (conductivity below 1 μS/cm). The commercial cerium oxide aqueous dispersion (Nanobyk-3810, 18 wt%, Byk Chemie) was dialyzed 4 times against deionized water employing Spectra/por 6 dialysis membranes (Spectrum Laboratories, MWCO 1000).

2.2. Synthesis of Dibenzyltrithiocarbonate (DBTTC)

Dibenzyltrithiocarbonate (DBTTC) was synthesized according to the same procedure as already described in the scientific literature[14,16].

2.3. Polymerizations

2.3.1. Synthesis of poly(BA-co-AA) RAFT oligomers

Details of the synthesis and characterization of poly(BA-*co*-AA) random copolymers are provided in the Supporting Information.

2.3.2. Synthesis of poly(BA-co-AMPS) and poly(BA-co-AA-co-AMPS) RAFT oligomers

Poly(BA-*co*-AMPS) random copolymers with different compositions were synthesized by copolymerization of butyl acrylate and 2-acrylamido-2-methyl propane sulfonic acid (AMPS) in dimethylsulfoxide (DMSO) at 70°C, employing AIBN as initiator and DBTTC as RAFT agent. A DBTTC:AIBN molar ratio of 3.3 was employed in order to achieve a good control over the polymerization reaction. For the syntheses of the poly(BA_5-*co*-$AMPS_5$) RAFT oligomer, a time-dependent ^1H NMR analysis was performed in parallel on a 0.6 mL sample of the reaction medium placed in a NMR tube with 3 capillaries containing deuterated benzene C_6D_6 and analyzed for 10 hours at 70°C in a 250 MHz Bruker NMR spectrometer. To obtain the macro-RAFT agents in their dry form for further analyses and emulsion polymerization reactions, a portion of each polymer solution was dried in a rotary evaporator and then overnight in a vacuum oven at 60°C. To remove the unreacted AMPS, copolymers were dissolved in 50mL water and dialyzed against a large volume (3L) of DI water in a Spectra/por 6 dialysis tubing (Spectrum Laboratories, MWCO 1000). The dry copolymer was then obtained by drying the solution in a rotary evaporator and overnight in a vacuum oven at 50°C. Stock aqueous solutions of poly(BA-*co*-AMPS) macro-RAFT agents were obtained by dissolving 0.5 g of oligomer in 100 mL DI water, in the presence of sodium hydroxide to achieve a neutral pH.

The same synthesis and purification procedures were followed for the RAFT terpolymerization of butyl acrylate, acrylic acid and AMPS.

Matrix Assisted Laser Desorption Ionization - Time of Flight – Mass Spectrometry (MALDI-ToF-MS) analyses of these poly(BA-*co*-AMPS) and poly(BA-*co*-AA-*co*-AMPS) RAFT oligomers are detailed in the Supporting Information.

2.3.3. Emulsion polymerizations

Emulsion copolymerization of styrene and methyl acrylate was carried out in the presence of amphiphatic macro-RAFT agents and cerium oxide particles according to the following procedure. The initial load containing the dialyzed cerium oxide aqueous dispersion and the RAFT oligomer diluted in deionized water, a mixture of the monomers (styrene and methyl acrylate in a 90:10 mass ratio / 88:12 molar ratio) and an aqueous initiator solution (VA-057, 4 g/L) were bubbled separately with argon during 30 min. The initial load was introduced in a 3-neck 250 mL double-walled reactor equipped with a condenser and maintained under argon atmosphere. Continuous stirring of the medium at 250 rpm was ensured by a 6-bladed stainless steel turbine impeller, and the temperature in the reactor was controlled with a continuous flow of thermostated water delivered by a MGW Lauda M3 circulating water bath. Once the reactor had reached the temperature of 60°C, a pulse of 10 mL of the initiator solution was injected into the reaction medium and the monomer feed via a Dosimat 765 dosing pump (Metrohm) was started and maintained for 4 hours at a rate of 42 μL/min (the emulsion polymerization process actually did not follow starved conditions and a retardation effect was noticed). Afterwards, the reactor was maintained at reaction temperature for an additional 2 hours.

2.4. Characterization

2.4.1. Molecular weight determination

Sulfonic acid groups were protected prior to Size Exclusion Chromatrography (SEC) analyses of poly(BA-*co*-AMPS) and poly(BA-*co*-AA-*co*-AMPS) copolymers: 40 mg of sample was dissolved in dimethylformamide (DMF) and an excess of trimethoxysilyl diazomethane was added (about 0.5 mL of a 2.0 M solution in heptane). The reaction was maintained for 3 hours in total. SEC with DMF as eluent, calibrated with poly(methyl

methacrylate) standards from Polymer Laboratories, was run with a Varian Prostar (model 210) pump at a flow rate of 0.8 mL.min^{-1} using two 300 mm long, mixed-D PL-gel 5 µm columns (molecular weight range: $2 \times 10^2 - 4 \times 10^5$ g.mol^{-1} from Polymer Laboratories) thermostated at 70°C, connected to a Shodex (model RI-101) refractometer detector. ^{1}H NMR analyses were carried out on a Brüker 400 MHz NMR spectrometer to determine monomer conversions (with the crude reaction products diluted in DMSO-d_6) and experimental molecular weights and compositions (with the dry copolymers dissolved in deuterium oxide, D_2O).

2.4.2. UV-visible spectrometry

25 mL aqueous solutions containing 4 g/L cerium oxide and macro-RAFT agent concentrations varying from 0 to 8 g/L were prepared (at pH 7) and stirred overnight in polyallomer tubes. The closed tubes were placed symmetrically in a rotor 70 Ti inside an Optima L-90K (Beckman Coulter) ultracentrifuge. After a cycle of 4 h at 40000 rpm at 20°C, 15 mL of the serum of each sample was collected.

UV-visible spectrometric measurements were performed on an Agilent 8453 UV-visible Spectroscopy System. Spectra were measured between 190 and 1100 nm, employing two different light sources: a deuterium lamp and a low-noise tungsten lamp. A temperature controller (HP Peltier 890904) was employed to maintain a constant temperature of 25°C. For each type of macro-RAFT agent, a calibration curve, giving the maximum absorbance (at 308 nm, specific for the trithiocarbonate function) as a function of the oligomer concentration in water (from 0.005 to 0.3 g/L) was plotted. UV-visible measurements were carried out on the serum solutions, diluted 10 or 100 times in order to fit the range of absorbance of the calibration curve. From this curve, the concentration of the free macro-RAFT agent present in

the serum could then be calculated, as well as the mass of RAFT oligomer adsorbed per gram of cerium oxide.

For analyses involving the poly(BA_5-*co*-AA_5) macro-RAFT agent, due to the incomplete solubility of the copolymer in water, even at neutral pH, a large amount of the stock solution was ultracentrifuged at 40000 rpm for 2 h beforehand in order to eliminate insoluble residues that could affect the adsorption process. ^{1}H NMR analyses performed on the serum showed no variation of the RAFT copolymer composition. No preliminary treatment was required when studying poly(BA-*co*-AMPS) and poly(BA-*co*-AA-*co*-AMPS) macro-RAFT agents, due to the complete solubility of these oligomers in water.

2.4.3. Dynamic Light Scattering

Latex particle size distributions and average particle diameters of CeO_2/poly(Sty-*co*-MA) hybrid latexes obtained from the poly(BA-*co*-AA) macro-RAFT agents were determined by dynamic light scattering (DLS) with a Zetasizer Nano ZS particle size analyzer (from Malvern). Latex particle size distributions and average particle diameters of CeO_2/poly(Sty-*co*-MA) hybrid latexes obtained from poly(BA-*co*-AMPS) and poly(BA-*co*-AA-*co*-AMPS) macro-RAFT agents were determined with a VASCO-3 particle size analyzer (from Cordouan technologies).

2.4.4. Cryo-TEM observations

The preparation of samples for cryo-TEM observations involved a vitrification procedure on a FEI Vitrobot Mark III. A 3 µL sample (about 5 wt% solid content) was applied to a Quantifoil grid (R 2/2, Quantifoil Micro Tools GmbH; glow discharged for 40 s just prior to use) within the environmental chamber of the Vitrobot and the excess liquid was blotted away. The sample was shot into melting ethane, immediately transferred to a

cryoholder (Gatan 626) and observed under low dose conditions at -170 °C. Cryo-TEM pictures were obtained using a FEI Tecnai 20, Sphera TEM microscope (LaB_6 filament, operating voltage of 200 kV).

3. Results and discussion

3.1. Synthesis and characterization of sulfonated macro-RAFT agents

Poly(BA-*co*-AMPS) copolymers with two different compositions and chain lengths were synthesized by RAFT copolymerization of butyl acrylate and AMPS at 70 °C in DMSO in the presence of AIBN as radical initiator and dibenzyl trithiocarbonate as chain transfer agent (Table 1). A ratio $[DBTTC]_0/[AIBN]_0$ of 3.3 was judged sufficient to favor the transfer to the RAFT agent and achieve a good control over the polymerization reaction, given that a few preliminary experiments carried out in presence of lower amounts of initiator resulted in too low monomer conversions (BA conversion < 90% and AMPS conversion < 60%).

Table 1. Polymerization recipes for the synthesis of poly(BA-*co*-AMPS) amphiphatic macro-RAFT agents.

Entry	Targeted macro-RAFT agent composition	BA (g)	AMPS (g)	DBTTC (g)	AIBN (g)	DMSO (g)
A1'	poly($BA_{7.5}$-*co*-$AMPS_{10}$)	1.73	3.74	0.524	0.090	54.29
A2'	poly(BA_5-*co*-$AMPS_5$)	1.86	2.98	0.839	0.143	53.99

In order to study the reactivity of butyl acrylate and AMPS, a time-dependent ^1H NMR study was employed to follow the course of the copolymerization of the two monomers. According to the evolution of the conversion of each monomer as a function of time and of the overall monomer conversion (Figure 1), AMPS reacted somewhat slower

than butyl acrylate. Nonetheless, the fact that the gradient structure (composition drift along the polymer chain) was not too much pronounced encouraged us to go on with this system for further experiments.

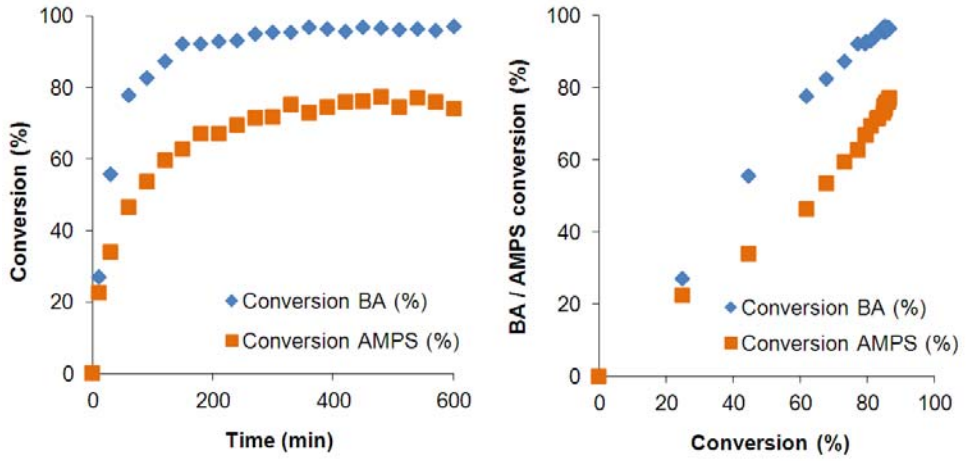

Figure 1. Butyl acrylate and AMPS conversions determined by ^{1}H NMR as a function of time (left) and as a function of the total monomer conversion (right) for the targeted copolymer composition poly(BA_5-*co*-$AMPS_5$).

Theoretical molecular weights of poly(BA-*co*-AMPS) copolymers were estimated from the equation:

$$M_{n,th} = M_{DBTTC} + [(m^0_{AMPS} \times X_{AMPS} + m^0_{BA} \times X_{BA}) / n^0_{DBTTC}] \qquad (6)$$

where m^0_{AMPS} and m^0_{BA} are the initial masses of AMPS and butyl acrylate respectively. X_{AMPS} and X_{BA} are the AMPS and BA conversions, n^0_{DBTTC} is the initial molar amount of RAFT agent and M_{DBTTC} corresponds to the RAFT agent molecular weight.

^{1}H NMR analyses carried out on the dry poly(BA-*co*-AMPS) copolymers dissolved in deuterium oxide (D_2O) were employed to determine their average molecular weights and compositions (Table 2). A fairly good agreement could be observed between the theoretical and experimental copolymer compositions and molecular weights, although molecular weights determined from ^{1}H NMR analyses were slightly higher than the predicted values.

Table 2. Characterization of poly(BA-*co*-AMPS) oligomers by ^{1}H NMR and SEC.

		Theoretical values		**^{1}H NMR results**				**SEC results**	
Entry	**Composition**	**$M_{n,\,th}$ (g/mol)**	**$F_{AMPS,th}$**	**X_{BA} (%)**	**X_{AMPS} (%)**	**$M_{n,\,NMR}$ (g/mol)**	**$F_{AMPS,NMR}$**	**$M_{n,\,SEC}$ (g/mol)**	**M_w/M_n**
A1'	poly($BA_{7.2}$-*co*-$AMPS_{7.6}$)	2740	0.52	95.8	75.6	3030	0.53	3820	1.28
A2'	poly($BA_{4.9}$-*co*-$AMPS_{3.8}$)	1690	0.44	97.8	76.2	1750	0.44	2550	1.30

Size exclusion chromatography performed on the oligomers, after substitution of sulfonic acid groups by a reaction with trimethylsilyl diazomethane, showed that poly(BA-*co*-AMPS) RAFT oligomers exhibited low polydispersity indices (PDI < 1.3), which evidenced that the DBTTC RAFT agent achieved a fairly good molecular weight control. Although molecular weights determined by SEC did not match theoretical values – as they were calculated against poly(methyl methacrylate) standards – the comparison of theoretical and SEC results followed a coherent trend.

The next series of experiments consisted in the RAFT terpolymerization of butyl acrylate, acrylic acid and AMPS (Table 3).

Table 3. Polymerization recipes for the synthesis of poly(BA-*co*-AA-*co*-AMPS) amphiphatic macro-RAFT agents.

Entry	Targeted macro-RAFT agent composition	BA (g)	AA (g)	AMPS (g)	DBTTC (g)	AIBN (g)	DMSO (g)
A1''	poly($BA_{7.5}$-*co*-AA_{10}-*co*-$AMPS_4$)	2.68	2.00	2.30	0.807	0.137	34.00
A2''	poly(BA_5-*co*-AA_5-*co*-$AMPS_4$)	2.16	1.19	2.76	0.970	0.164	34.00

Theoretical molecular weights were calculated according to the following equation:

$$M_{n,th} = M_{DBTTC} + [(m^0_{AMPS} \times X_{AMPS} + m^0_{AA} \times X_{AA} + m^0_{BA} \times X_{BA}) / n^0_{DBTTC}] \quad (7)$$

where m^0_{AMPS}, m^0_{AA} and m^0_{BA} are the initial masses of AMPS, acrylic acid and butyl acrylate, respectively. X_{AMPS}, X_{AA} and X_{BA} are the AMPS, AA and BA conversions, n^0_{DBTTC} is the initial molar amount of RAFT agent and M_{DBTTC} corresponds to the RAFT agent molecular weight.

^{1}H NMR analyses carried out on the crude reaction product and the dry terpolymers (in DMSO-d_6 and D_2O, respectively) were employed to determine the monomer conversions and the terpolymer average compositions and molecular weights, respectively (Table 4).

Table 4. Characterization of poly(BA-*co*-AA-*co*-AMPS) oligomers by ^{1}H NMR.

		Theoretical values			^{1}H NMR analyses						SEC results	
Entry	Composition	$M_{n,th}$ (g/mol)	$F_{AA,th}$	$F_{AMPS,th}$	X_{BA} (%)	X_{AA} (%)	X_{AMPS} (%)	$M_{n,NMR}$ (g/mol)	$F_{AA,NMR}$	$F_{AMPS,NMR}$	$M_{n,SEC}$ (g/mol)	M_w/M_n
A1''	poly($BA_{7.5}$-*co*-$AA_{9.8}$-*co*-$AMPS_{3.5}$)	2660	0.47	0.17	99.5	98.3	90.2	2830	0.46	0.17	4176	1.25
A2''	poly($BA_{5.0}$-*co*-$AA_{4.9}$-*co*-$AMPS_{3.6}$)	2010	0.36	0.27	99.3	97.5	88.2	2110	0.43	0.21	3350	1.23

A good agreement was found between theoretical and experimental molecular weights, although the final compositions of each monomer did not completely match the expected values. SEC analyses showed a narrow molecular weight distribution (with polydispersity indices lower than 1.3), despite the discrepancy between the theoretical molecular weights and the experimental values calculated against poly(methyl methacrylate) standards. Time-dependent ^{1}H NMR analyses were not carried out to study the terpolymerization of the three monomers. However, based on previous experiments carried out on poly(BA-*co*-AMPS) copolymer and on the fact that butyl acrylate and acrylic acid were shown to give random copolymers[12,19,20] (see also Supporting Information), we may reasonably assume that the polymers would display a gradient structure (slight composition drift along the chains), with butyl acrylate/acrylic acid rich "tails" and an AMPS rich "center". MALDI-ToF-MS analyses of the copolymers and terpolymers were also consistent with the expected macro-RAFT agent structures (see Supporting Information). Figure 2 illustrates the structures expected for the RAFT copolymers and terpolymers based on the characterization results obtained on the different classes of macro-RAFT agents.

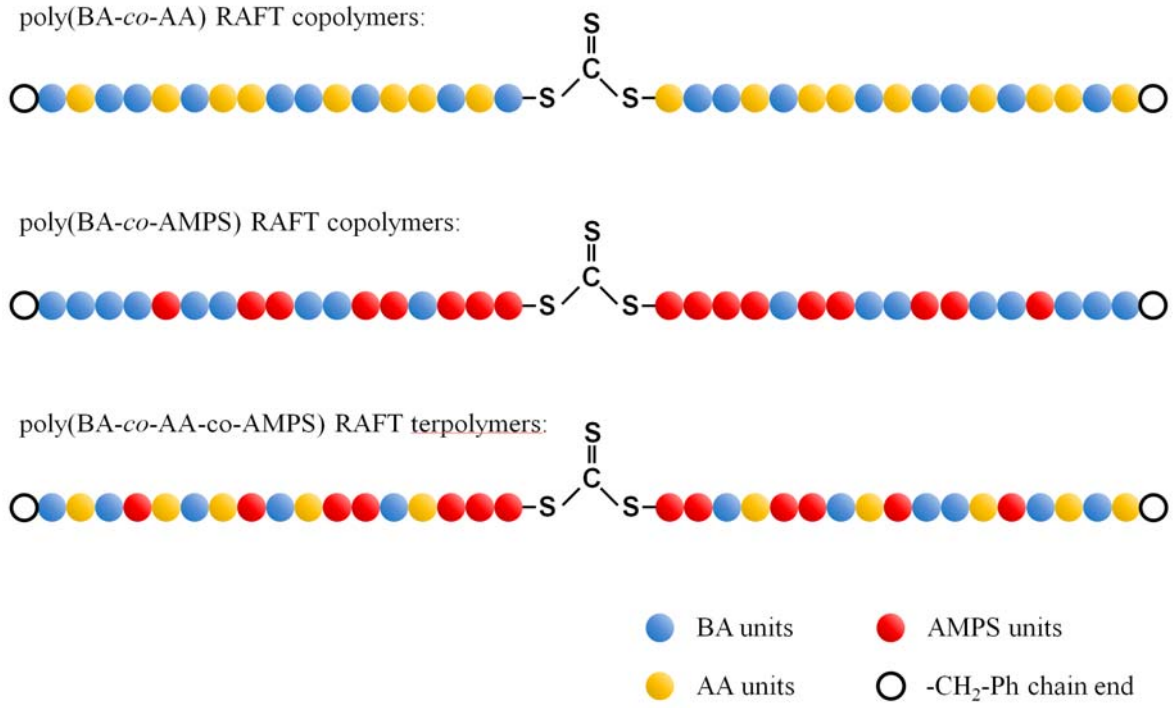

Figure 2. Schematic view of the structures of amphiphatic macro-RAFT agents.

3.2. Adsorption of amphiphatic macro-RAFT agents

To characterize quantitatively the adsorption of poly(BA-*co*-AA) copolymers, solutions of the poly(BA_5-*co*-AA_5) macro-RAFT agent were prepared in the presence of cerium oxide and ultracentrifuged at 40000 rpm for 4h to isolate the supernatant and plot the corresponding adsorption isotherms via UV-visible spectrometric measurements performed on the serum (Figure 3). We could indeed take advantage of the specific absorption of the C=S bond of trithiocarbonate functions taking place between 265 and 365 nm (with a maximum at 308 nm) to determine the concentration of the macro-RAFT agent remaining in the aqueous phase and, by means of a mass balance, estimate the mass of RAFT copolymer adsorbed per gram of cerium oxide. This calculation required the approximation that the adsorption process was independent of the length and composition of polymer chains, which may in reality not be exactly the case. It was also based on the assumption that no desorption

of the RAFT copolymer from the cerium oxide surface occurred during the ultracentrifugation procedure.

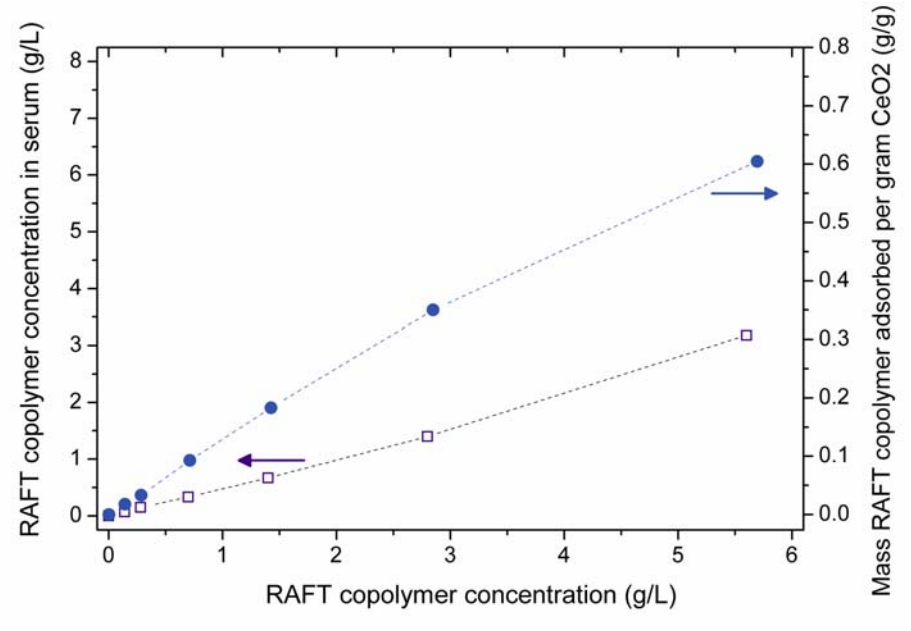

Figure 3. Adsorption of the poly(BA_5-*co*-AA_5) macro-RAFT agent at the surface of cerium oxide particles evidenced by UV-visible spectrometry.

From this diagram, it could be concluded that, within the studied range of concentrations, the adsorption of the macro-RAFT agent occurred successfully at the surface of nanoceria, but with a large percentage of copolymer – between 50 and 60% – remaining in the aqueous phase. Similar results were reported by Nguyen et al.[16] in the case of a poly(BA_5-*co*-AA_{10}) macro-RAFT agent adsorbed at the surface of titanium dioxide: they showed that roughly 75% of the RAFT oligomer remained dissolved in the aqueous phase. However, they proved that these aqueous phase macro-RAFT agents did not affect the efficient encapsulation of titanium dioxide and hardly led to secondary nucleation.

UV-visible spectroscopic analyses carried out on supernatants of ultracentrifugated cerium oxide/poly($BA_{4.9}$-*co*-$AMPS_{3.8}$) dispersions showed a very different trend compared to the case of poly(BA-*co*-AA) RAFT copolymers (Figure 4). Indeed, the macro-RAFT agent mostly remained dissolved in the water phase and hardly any RAFT copolymer adsorbed at the cerium oxide surface. We cannot exclude that desorption of some poly(BA-*co*-AMPS) occurred to some extent during the ultracentrifugation process. Nevertheless this result clearly shows that, contrary to carboxylic acid groups, sulfonate groups display a very weak affinity towards the CeO_2 surface.

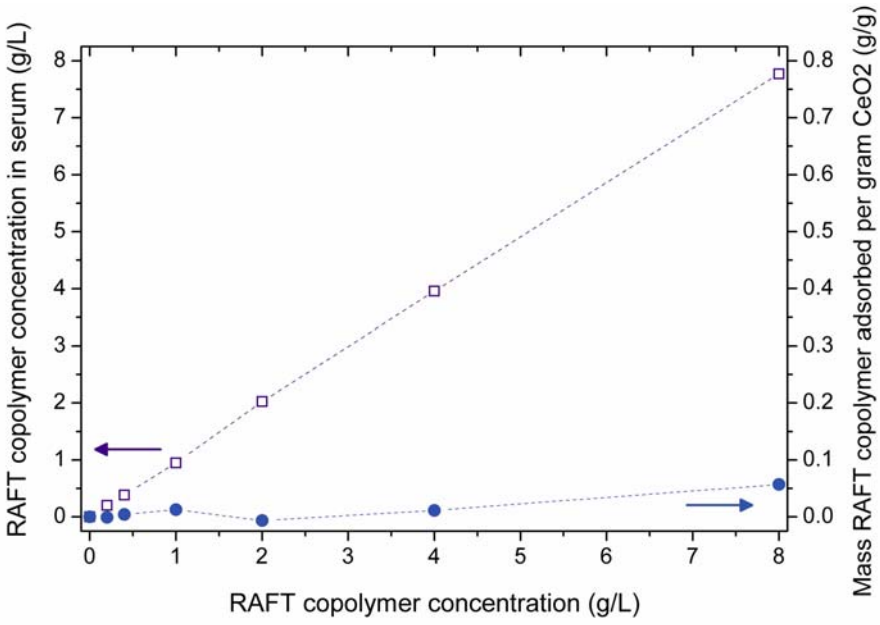

Figure 4. Adsorption of the poly($BA_{4.9}$-*co*-$AMPS_{3.8}$) macro-RAFT agent at the surface of cerium oxide particles evidenced by UV-visible spectrometry.

The same experimental procedure was employed to study the adsorption of the poly($BA_{5.0}$-*co*-$AA_{4.9}$-*co*-$AMPS_{3.6}$) RAFT oligomer at the surface of nanoceria. The adsorption isotherm represented in Figure 5 shows that the incorporation of acrylic acid units in the RAFT terpolymer resulted in a slight increase of the mass of macro-RAFT agent

adsorbed per gram of cerium oxide compared to the case of the poly($BA_{4.9}$-*co*-$AMPS_{3.8}$) RAFT copolymer. Nevertheless, this value remained very low compared to the mass of poly(BA_5-*co*-AA_5) oligomer adsorbed per gram of cerium oxide. In this case too, the ultracentrifugation step employed to characterize the adsorption process could have induced the desorption of the sulfonated RAFT terpolymers towards the serum phase and led to an underestimated value of the percentage of macro-RAFT agent present at the cerium oxide surface.

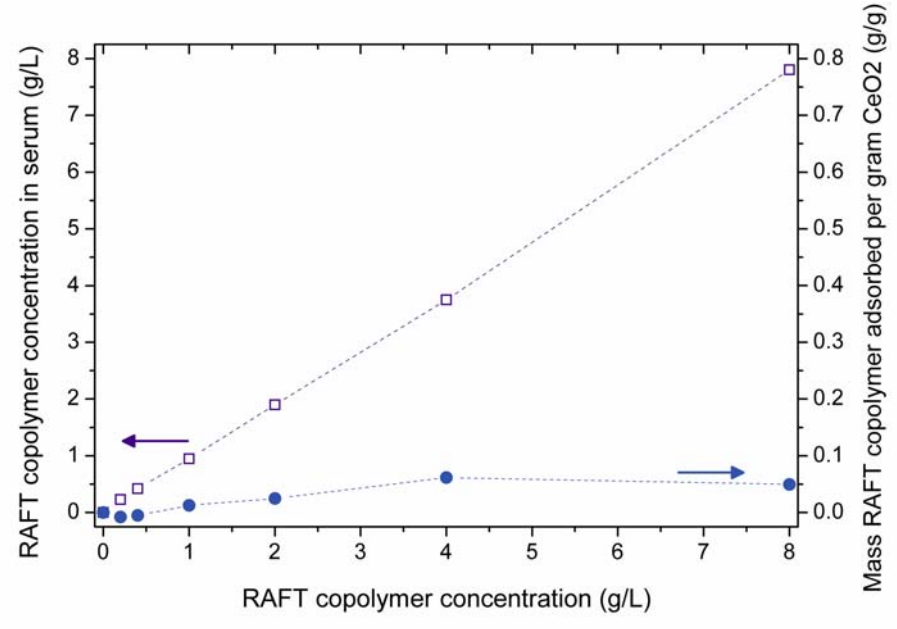

Figure 5. Adsorption of the poly($BA_{5.0}$-*co*-$AA_{4.9}$-*co*-$AMPS_{3.6}$) macro-RAFT agent at the surface of cerium oxide particles evidenced by UV-visible spectrometry.

A remarkable advantage of sulfonated macro-RAFT agents compared to RAFT copolymers of butyl acrylate and acrylic acid was their very good solubility in water. Indeed, while a slow addition of a sodium hydroxide solution and a vigorous stirring were required to solubilize (sometimes even incompletely) poly(BA-*co*-AA) copolymers at neutral pH, poly(BA-*co*-AMPS) and poly(BA-*co*-AA-*co*-AMPS) macro-RAFT agents were immediately

soluble at acidic pH, owing to the stronger acidity of sulfonic acid groups (pKa < 1) compared to carboxylic acid groups (pKa ~ 4.8). At the same time this higher water solubility of the sulfonated macro-RAFT agents contributes to their lower adsorption on the cerium oxide particles.

3.3. Surfactant-free synthesis of CeO_2/poly(Sty-co-MA) hybrid latexes

Reactions of emulsion copolymerization of styrene and methyl acrylate (in a 90:10 mass ratio) were carried out at neutral pH in the presence of ceria employing different types and compositions of macro-RAFT agents (Table 5).

Table 5. Recipes for the emulsion copolymerization of styrene and methyl acrylate in the presence of nanoceria and amphiphatic macro-RAFT agents.

Entry	Macro-RAFT agent composition	Cerium oxide dispersion (g)	Macro-RAFT agent (g)	VA-057 (g)	Water (g)	Styrene/methyl acrylate (g/g)
B1	poly($BA_{7.3}$-*co*-$AA_{9.8}$)	3.16 [a)]	0.195	0.0395	71.00	8.16 / 0.91
B2	poly($BA_{4.8}$-*co*-$AA_{4.9}$)	3.16 [a)]	0.195	0.0395	73.00	8.16 / 0.91
B1'	poly($BA_{7.2}$-*co*-$AMPS_{7.6}$)	2.17 [b)]	0.120	0.024	43.10	5.15 / 0.57
B2'	poly($BA_{4.9}$-*co*-$AMPS_{3.8}$)	2.14 [b)]	0.120	0.022	40.18	4.99 / 0.55
B1''	poly($BA_{7.5}$-*co*-$AA_{9.8}$-*co*-$AMPS_{3.5}$)	2.20 [b)]	0.165	0.022	41.04	5.15 / 0.57
B2''	poly($BA_{5.0}$-*co*-$AA_{4.9}$-*co*-$AMPS_{3.6}$)	2.21 [b)]	0.188	0.033	42.11	5.15 / 0.57

[a)] CeO_2 content of the dispersion: 12.3 wt%.

[b)] CeO_2 content of the dispersion: 10.9 wt%.

In all cases, a solid content of 12 wt% and a 4 wt% cerium oxide content (respective to the dry polymer) were targeted. A zwitterionic radical initiator (VA-057) was used to

initiate the polymerization. High monomer conversions could be achieved in most cases and stable latexes were obtained (Table 6).

Table 6. Characterization results of CeO_2/poly(styrene-*co*-methyl acrylate) latexes.

Entry	Macro-RAFT agent composition	X_M (%)	D_P (nm)	Polydispersity index	N^0_{CeO2} (x 10^{-16})[a]	N^f_P (x 10^{-16})[a]	N^0_{CeO2}/N^f_P
B1	poly($BA_{7.3}$-*co*-$AA_{9.8}$)	91.1	56	0.16	20	8.7	2.3
B2	poly($BA_{4.8}$-*co*-$AA_{4.9}$)	86.2	83	0.21	20	2.5	8.1
B1'	poly($BA_{7.2}$-*co*-$AMPS_{7.6}$)	81.1	51	0.15	12	6.5	1.9
B2'	poly($BA_{4.9}$-*co*-$AMPS_{3.8}$)	75.4	50	0.25	12	6.0	2.0
B1''	poly($BA_{7.5}$-*co*-$AA_{9.8}$-*co*-$AMPS_{3.5}$)	85.2	48	0.11	13	8.0	1.6
B2''	poly($BA_{5.0}$-*co*-$AA_{4.9}$-*co*-$AMPS_{3.6}$)	84.3	48	0.19	13	8.1	1.6

[a] N^0_{CeO2} is the initial number of CeO_2 particles in the reactor, N^f_P is the total number of latex particles in the reactor at the end of the polymerization.

Cryo-TEM observations performed on CeO_2/poly(Sty-*co*-MA) latex samples obtained from poly(BA-*co*-AA) RAFT copolymers already showed that this class of macro-RAFT agents could lead to the efficient incorporation of cerium oxide nanoclusters into hybrid particles (Figure 6). However, we assumed that this type of amphiphatic RAFT oligomers did not provide hybrid particle precursors a sufficient colloidal stability and the formation of a certain amount of larger latex particles decorated with several CeO_2 nanoclusters was attributed to the partial coalescence of these hybrid precursors[16].

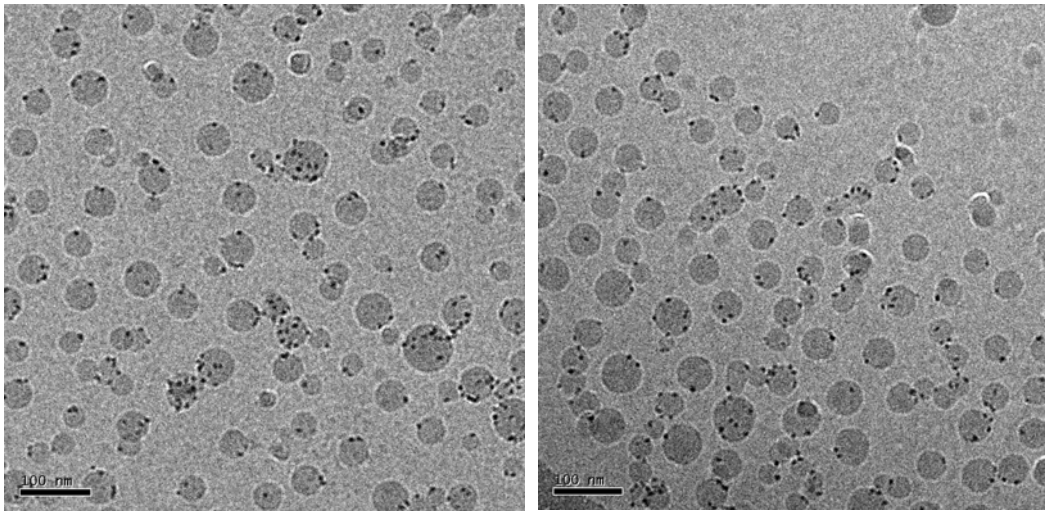

Figure 6. Cryo-TEM picture of CeO_2/poly(styrene-*co*-methyl acrylate) hybrid latexes B1 (left) and B2 (right) obtained in the presence of poly($BA_{7.3}$-*co*-$AA_{9.8}$) and poly($BA_{4.8}$-*co*-$AA_{4.9}$) macro-RAFT agents, respectively.

The initial number of cerium oxide particles (N^0_{CeO2}) and the final number of hybrid particles (N^f_P) were calculated from volume mean particle diameters via the equations:

$$N^0_{CeO2} = 6 \times m^0_{CeO2} / (\pi \times \rho_{CeO2} \times D_{CeO2}{}^3) \quad (1)$$

$$N^f_P = 6 \times [(m^0_{Sty} + m^0_{MA}) \times X_M + m^0_{RAFT\ copolymer}] / (\pi \times \rho_{polymer} \times D_P{}^3) \quad (2)$$

Where m^0_{CeO2} stands for the initial mass of cerium oxide, ρ_{CeO2} for the density of cerium oxide (ρ_{CeO2} = 7.13 g/cm^3), D_{CeO2} for the volume mean diameter of ceria (D_{CeO2} = 8 nm) and m^0_{Sty} and m^0_{MA} for the initial masses of styrene and methyl acrylate, respectively. X_M is the overall monomer conversion, $m^0_{RAFT\ copolymer}$ the initial mass of macro-RAFT agent, $\rho_{polymer}$ the polymer density (assuming $\rho_{polymer} \approx \rho_{polystyrene}$ = 1.05 g/cm^3) and D_P the hybrid particle volume mean diameter. The contribution of cerium oxide in the calculation of the final number of hybrid particles can be neglected since the dry cerium oxide content did not exceed 4 wt%.

At first sight, average particle diameters determined by Dynamic Light Scattering suggested that the presence of sulfonate groups in poly(BA-*co*-AMPS) and poly(BA-*co*-AA-*co*-AMPS) macro-RAFT agent chains resulted in a lower particle size and, accordingly, a lower average number of cerium oxide nanoclusters per latex particle, regardless of the RAFT oligomer compositions (Table 6). However, cryo-TEM observations revealed that poly(BA-*co*-AMPS) RAFT copolymers did not lead to any incorporation of cerium oxide nanoparticles into latex particles (Figure 7). This result is in agreement with adsorption isotherms measured for this type of macro-RAFT agent: given that most poly(BA-*co*-AMPS) RAFT copolymer chains remained in the aqueous phase, their chain extension may have led to the formation of micelles and to the subsequent nucleation of CeO_2-free polymer particles. We could thus conclude that the mere presence of sulfonated groups in the macro-RAFT agent chain was not sufficient to promote a seeded emulsion polymerization mechanism starting from the cerium oxide surface.

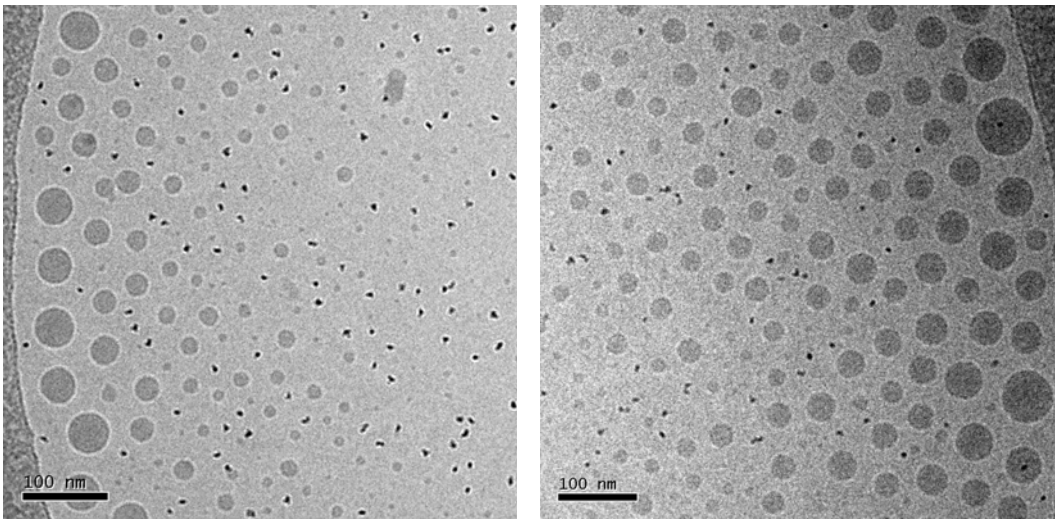

Figure 7. Cryo-TEM observations of CeO_2/poly(styrene-*co*-methyl acrylate) hybrid latexes B1' (left) and B2' (right), obtained in the presence of poly($BA_{7.2}$-*co*-$AMPS_{7.6}$) and poly($BA_{4.9}$-*co*-$AMPS_{3.8}$) macro-RAFT agents, respectively.

Therefore the presence of carboxylic acid groups in the macro-RAFT agent chain appeared critical to direct the polymerization reaction to the cerium oxide surface. RAFT terpolymers combining butyl acrylate, acrylic acid and AMPS units were thus considered as an alternative to the two previous classes of amphiphatic RAFT copolymers: acrylic acid units, due to their strong complexing activity towards the cerium oxide surface[21], could promote the adsorption of the macro-RAFT agent at the cerium oxide surface, while AMPS units, bearing sulfonic acid groups, could provide hybrid particles a sufficient colloidal stability during their growth. Cryo-TEM observations evidenced that poly(BA-*co*-AA-*co*-AMPS) terpolymers enabled the efficient formation of CeO_2/poly(Sty-*co*-MA) hybrid particles with a very good distribution of cerium oxide nanoclusters between latex particles (Figure 8). Indeed, most hybrid particles displayed a "single-headed" snowman morphology, strongly suggesting that sulfonic acid helped stabilizing the growth of hybrid particle precursors throughout the whole emulsion polymerization reaction.

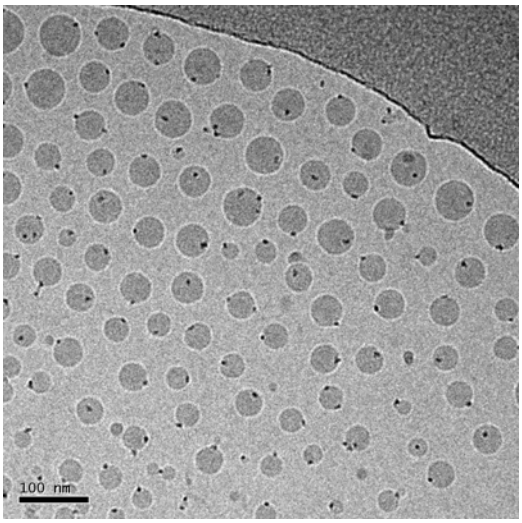

Figure 8. Cryo-TEM picture of the CeO_2/poly(styrene-*co*-methyl acrylate) hybrid latex B2'' obtained in the presence of the poly($BA_{5.0}$-*co*-$AA_{4.9}$-*co*-$AMPS_{3.6}$) macro-RAFT agent.

Intriguingly, considering the very low proportion of RAFT terpolymer adsorbed at the oxide surface – roughly 5 wt% according to adsorption isotherms determined for this system (Figure 4) – such a high efficiency of hybrid particle formation was unexpected. We could thus conclude that a high degree of adsorption of amphiphatic macro-RAFT agents at the oxide surface was not a prerequisite for a high incorporation efficiency, and led us to reconsider the actual mechanism of formation of hydrophobic domains at the cerium oxide surface when poly(BA-*co*-AA-*co*-AMPS) RAFT terpolymers are employed: we believe that, when adding hydrophobic monomer units during the emulsion polymerization reaction, the macro-RAFT agents initially present in the aqueous phase acquired an increasing hydrophobicity and migrated towards the cerium oxide surface where they could displace some citrate ligands of the CeO_2 nanoparticles. These poly(BA-*co*-AA-*co*-AMPS) RAFT terpolymers located at the CeO_2 surface underwent further chain extension, promoting the growth of polymer domains and contributing to the colloidal stability of the hybrid latex.

The outstanding feature of this process is that these macro-RAFT agents, when adding monomer units, became sufficiently hydrophobic to promote the polymerization reaction at the oxide/water interface and stabilize the hybrid particle growth, but not surface active enough to encourage the formation of a second crop of polymer particles by secondary nucleation. Comparing the results obtained between the poly(BA-*co*-AMPS) (massive renucleation) and poly(BA-*co*-AA-*co*-AMPS) (efficient formation of hybrid particles), the differentiation between the two mechanisms seems, as expected, closely related to the presence of acrylic acid monomer units bearing carboxylic acid groups which are more prone to ligand exchange of CeO_2 ligands than sulfonic acid groups of AMPS.

4. Conclusions

Two types of amphiphatic sulfonated macro-RAFT agents were synthesized, employing butyl acrylate as hydrophobic monomer, 2-acrylamido-2-methylpropane sulfonic acid (AMPS) and acrylic acid as hydrophilic monomers and dibenzyl trithiocarbonate as chain transfer agent. ^{1}H NMR and SEC analyses suggested that a fairly good control of the molecular weights was achieved during the copolymerization reactions, while MALDI-ToF-MS analyses of poly(BA-*co*-AMPS) and poly(BA-*co*-AA-*co*-AMPS) macro-RAFT agents confirmed a good preservation of the trithiocarbonate chain-functionality. Due to the faster incorporation of butyl acrylate units into the polymer chains, compared to AMPS units, we could reasonably assume that both types of sulfonated oligomers displayed gradient structures with AMPS-richer centers.

UV-visible spectroscopic analyses carried out on the serum of ultracentrifugated solutions of macro-RAFT agents and nanoceria led to very different conclusions depending on the type of oligomers employed: while the adsorption of 50 to 60 wt% of poly(BA-*co*-AA) copolymers successfully occurred at the surface of cerium oxide nanoparticles, both types of sulfonated RAFT oligomers seemed to display a very low affinity towards the cerium oxide surface.

Surfactant-free emulsion polymerization reactions carried out in the presence of sulfonated macro-RAFT agents led to the formation of stable latexes with high monomer conversions and average particle diameters of about 50 nm. Observations of the resulting particles by cryo-TEM showed that the mere presence of sulfonated groups in the macro-RAFT agent was not sufficient to incorporate nanoceria into the final latex. The best compromise was found, between a high efficiency of hybrid particle formation and a good distribution of cerium oxide nanoclusters between latex particles, by combining butyl acrylate, acrylic acid and AMPS units: while carboxylic acid functions provided a high

affinity towards the cerium oxide surface, sulfonic acid groups enhanced the colloidal stability of "single-headed" snowman particles all along the polymerization reaction.

Beyond the fact that sulfonated RAFT terpolymers clearly enabled a better control of the morphology of cerium oxide-based hybrid latexes and confirmed our assumptions regarding the mechanism of hybrid particle formation, these results also lead us to a more general conclusion applicable to the incorporation of various types of inorganic particles into polymer latexes: the amphiphatic nature of a macro-RAFT agent is not a sufficient condition to allow the efficient formation of hybrid latexes, since it requires the presence of functions, such as carboxylic groups, displaying a complexing activity towards the metal oxide surface.

Acknowledgements

The authors wish to thank Rinske Knoop for her experimental support on cryo-TEM observations, Byk Chemie for the supply of cerium oxide dispersions, Solvay for funding this research project, and the French Ministry of Education and Research for the ANRT grant CIFRE N°261/2008 as well as for the research grant ANR-2010-RMNP-005-05.

Appendix A: Supplementary material

Supplementary data associated with this article can be found, in the online version, at http://dx.doi.org/10.1016/j.cis.2013.xxxxx.

References

[1] E. Bourgeat-Lami, M. Lansalot, Adv. Polym. Sci. 233 (2010) 53.

[2] E. Bourgeat-Lami, E. Duguet, "Polymer Encapsulation of Inorganic Particles", in Functional Coatings by Polymer Microencapsulation, S.K. Ghosh, Ed., Wiley-VCH Verlag GmbH & Co. KGaA, Weinheim, 2006, 85.

[3] J. Lemaire, D. Petta, O. Touret *EP599717A1*, 1994.

[4] A. Trovarelli, Catal. Rev. - Sci. Eng. 38 (1996) 439.

[5] R. V. Horrigan, ACS Symp. Ser. 164 (1981) 95.

[6] R. T. Dirstine, R. N. Blumenthal, T. F. Kuech, J. Electrochem. Soc. 126 (1979) 264.

[7] H. J. Beie, A. Gnoerich, Sens. Actuators, B B4 (1991) 393.

[8] T. Masui, K. Fujiwara, K.-I. Machida, G.-Y. Adachi, T. Sakata, H. Mori, Chem. Mater. 9 (1997) 2197.

[9] S. Tsunekawa, T. Fukuda, A. Kasuya, J. Appl. Phys. 87 (2000) 1318.

[10] S. Tsunekawa, J.-T. Wang, Y. Kawazoe, A. Kasuya, J. Appl. Phys. 94 (2003) 3654.

[11] B. Charleux, F. D'Agosto, G. Delaittre, Adv. Polym. Sci. 233 (2010) 125.

[12] D. Nguyen, H. S. Zondanos, J. M. Farrugia, A. K. Serelis, C. H. Such, B. S. Hawkett, Langmuir 24 (2008) 2140.

[13] D. Nguyen, C. Such, B. Hawkett, J. Polym. Sci., Part A: Polym. Chem. 50 (2011) 346.

[14] S. I. Ali, J. P. A. Heuts, B. S. Hawkett, A. M. Van Herk, Langmuir 25 (2009) 10523.

[15] P. Das, J. P. Claverie, J. Polym. Sci., Part A: Polym. Chem. 50 (2012) 2802.

[16] J. Garnier, J. Warnant, P. Lacroix-Desmazes, P.-E. Dufils, J. Vinas, Y. Vanderveken, A. M. van Herk, Macromol. Rapid Commun. 33 (2012) 1388.

[17] N. Zgheib, J.-L. Putaux, A. Thill, E. Bourgeat-Lami, F. D'Agosto, M. Lansalot, Polym. Chem. 4 (2013) 607.

[18] M. Aguirre, M. Paulis, J. R. Leiza, J. Mater. Chem. A 1 (2013) 3155.

[19] B. Vollmert, Angew. Makromol. Chem. No. 3 (1968) 1.

[20] T. R. Paxton, J. Polym. Sci., Part B: Polym. Lett. 1 (1963) 73.

[21] A. Sehgal, Y. Lalatonne, J. F. Berret, M. Morvan, Langmuir 21 (2005) 9359.

DOI: 10.1016/j.jcis.2013xxxxx

Supporting Information:

Sulfonated macro-RAFT agents for the surfactant-free synthesis of cerium oxide-based hybrid latexes

Jérôme Garnier[b], Jérôme Warnant[b], Patrick Lacroix-Desmazes[b,*], Pierre-Emmanuel Dufils[c], Jérôme Vinas[d], and Alex van Herk[a,*]

[a] *Institute of Chemical and Engineering Sciences, 1 Pesek Road, 627833 Singapore and Polymer Reaction Engineering group, Eindhoven University of Technology, P.O. Box 513, 5600 MB Eindhoven, The Netherlands.*
[b] *Institut Charles Gerhardt (ICG), UMR5253 CNRS/UM2/ENSCM/UM1, Ingénierie et Architectures Macromoléculaires (IAM), Ecole Nationale Supérieure de Chimie de Montpellier, 8 rue de l'Ecole Normale, 34296 Montpellier Cedex 5, France.*
[c] *High Barrier Polymers – Solvay Specialty Polymers – Avenue de la République, 39500 Tavaux, France.*
[d] *High Barrier Polymers – Solvay Specialty Polymers – Solvay Campus – Rue de Ransbeek 310, B-1120 Brussels, Belgium.*

* Corresponding authors:
Fax: +31 40 246 3966; E-mail address: A.M.v.Herk@tue.nl (A.M. van Herk)
Fax: +33 467 14 72 20; E-mail address: patrick.lacroix-desmazes@enscm.fr (P. Lacroix-Desmazes)

---

1. Synthesis and characterization of poly(BA-*co*-AA) copolymers

1.1. Synthesis of poly(BA-co-AA) RAFT oligomers

Poly(BA-*co*-AA) random copolymers with two different compositions were synthesized by copolymerization of butyl acrylate and acrylic acid in 1,4-dioxane at 70°C, employing AIBN as initiator and DBTTC as RAFT agent (Table SI.1). A DBTTC:AIBN molar ratio of 11 was employed in order to favor the transfer to the RAFT agent and achieve a good control over the polymerization reaction. To obtain the macro-RAFT agents in their dry form for further analyses and emulsion polymerization reactions, a portion of each polymer solution was dried overnight in a vacuum oven at 50°C. Stock aqueous solutions of poly(BA-*co*-AA) macro-RAFT agents were obtained by dissolving 0.5 g of oligomer in 100 mL DI water, in the presence of sodium hydroxide to achieve a neutral pH.

Table SI.1. Polymerization recipes for the synthesis of poly(BA-*co*-AA) amphiphatic macro-RAFT agents.

Entry	Targeted macro-RAFT agent composition	BA (g)	AA (g)	DBTTC (g)	AIBN (g)	1,4-dioxane (g)
A1	poly($BA_{7.5}$-*co*-AA_{10})	12.10	9.12	3.65	0.196	25.29
A2-1	poly(BA_5-*co*-AA_5)	10.60	6.03	4.80	0.238	24.95
A2-2	poly(BA_5-co-AA_5)	10.60	6.00	4.80	0.238	22.00

1.2. Characterization of poly(BA-co-AA) RAFT oligomers

1.2.1. Molecular weight determination

For poly(BA-*co*-AA) RAFT copolymers, size exclusion chromatography was performed on a system equipped with a Waters 1515 isocratic HPLC pump, a Waters 2707 autosampler, a Waters 2414 refractive index detector (35°C) and a PSS SDV 5µ guard column followed by 2 SDV 5µ, 500 Å (8 × 300 mm) columns in series at 40°C. Tetrahydrofuran with 1 vol% acetic acid was used as eluent at a flow rate of 1.0 $mL.min^{-1}$. The molecular weights were calculated against polystyrene standards (Polymer Laboratories, M_P = 580 $g.mol^{-1}$ up to M_P = 21000 $g.mol^{-1}$).

^1H NMR analyses performed on a Varian 400 MHz spectrometer (Figure SI.1) were employed to determine monomer conversions (with the crude reaction products diluted in DMSO-d_6) and the oligomers average molecular weights ($M_{n,\ NMR}$) and molar compositions ($F_{AA,\ NMR}$) (with the dry copolymers dissolved in DMSO-d_6).

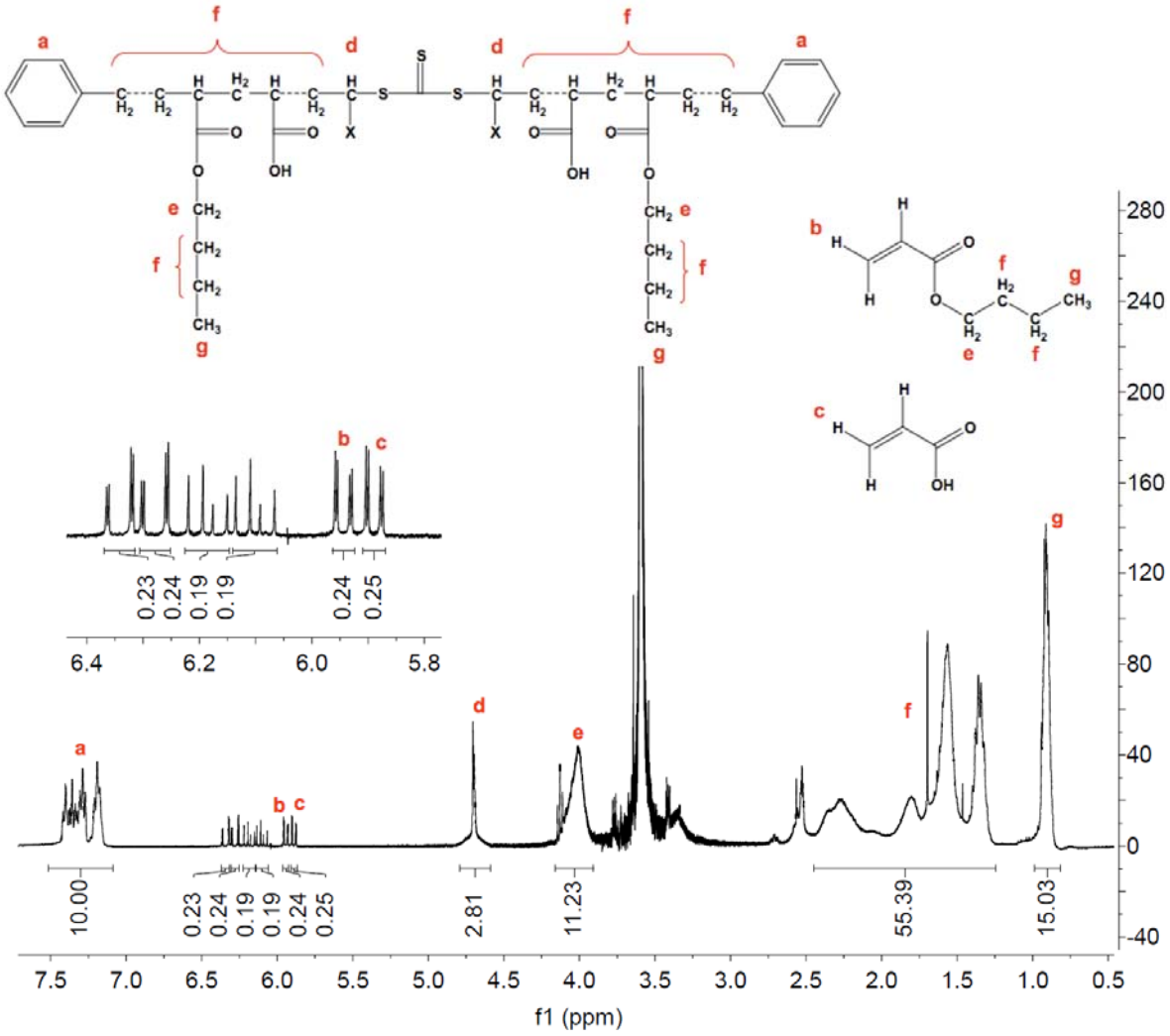

Figure SI.1. ^{1}H NMR spectrum and corresponding integration peaks of the poly(BA-*co*-AA) RAFT copolymer A2-1 with a BA_5-*co*-AA_5 targeted composition (crude reaction product diluted in DMSO-d_6).

Theoretical molecular weights were calculated via the following equation:

$$M_{n,th} = M_{DBTTC} + [(m^0_{BA} \times X_{BA} + m^0_{AA} \times X_{AA}) / n^0_{DBTTC}] \quad (1)$$

where m^0_{BA} and m^0_{AA} are the initial masses of butyl acrylate and acrylic acid, respectively, X_{BA} and X_{AA} the monomer conversions, n^0_{DBTTC} the initial moles of RAFT agent and M_{DBTTC} corresponds to the RAFT agent molecular weight.

Comparison of characterization results collected in Table SI.2 showed that experimental molecular weights were in general in good agreement with targeted values. However, some molecular weight discrepancies were observed concerning Size Exclusion Chromatography results, possibly due to interactions between carboxylic acid units and the SEC column that were not completely avoided by the use of small amounts of acetic acid in the THF eluent. Nevertheless, low PDI values obtained in all cases tended to confirm the controlled character of these polymerization reactions. Average compositions calculated from ^{1}H NMR results also matched the targeted values.

Table SI.2. Characterization of poly(BA-*co*-AA) oligomers by ^{1}H NMR and SEC.

		Theoretical values		**^{1}H NMR results**				**SEC results**	
Entry	**Composition**	**$M_{n,th}$ (g/mol)**	**$F_{AA,th}$**	**X_{BA} (%)**	**X_{AA} (%)**	**$M_{n,NMR}$ (g/mol)**	**$F_{AA,NMR}$**	**$M_{n,SEC}$ (g/mol)**	**M_w/M_n**
A1	poly($BA_{7.3}$-*co*-$AA_{9.8}$)	1940	0.57	97.5	97.7	1980	0.58	2060	1.28
A2-1	poly($BA_{4.8}$-*co*-$AA_{4.9}$)	1260	0.50	95.8	96.4	1300	0.51	1570	1.28

1.2.2. ^{1}H NMR kinetic analyses of the RAFT copolymerization of butyl acrylate and acrylic acid

The synthesis of the poly(BA_5-*co*-AA_5) macro-RAFT agent was repeated (experiment A2-2) to follow the conversions of both monomers against time. Samples were taken regularly and analyzed by ^{1}H NMR. The integration peak **a** corresponding to aromatic protons of benzyl chain ends was taken as an internal standard and the integrations of peaks **b**

and **c** (integrating for protons of butyl acrylate and acrylic acid respectively) (Figure SI.1) were used to calculate the conversions of the two monomers as a function of time:

$$X_{BA,\,t}\,(\%) = (b_{t=0} - b_t) \times 100 / b_{t=0} \qquad (2)$$

$$X_{AA,\,t}\,(\%) = (c_{t=0} - c_t) \times 100 / c_{t=0} \qquad (3)$$

where $X_{BA,\ t}$ and $X_{AA,t}$ are the conversions of butyl acrylate and acrylic acid respectively at time t, $b_{t=0}$, $c_{t=0}$ the integration values of peaks **b** and **c** at initial time and b_t and c_t are the integration values of peaks **b** and **c** at time t.

From these calculations, the conversions of the two monomers could be plotted as a function of time and as a function of the total monomer conversion (Figure SI.2). Although butyl acrylate seemed to be incorporated slightly faster than acrylic acid into the RAFT polymer chains at the initial stage of the reaction, we may still conclude that overall the two monomers copolymerized randomly. We may thus expect a very low proportion of blocky structures in poly(BA-*co*-AA) macro-RAFT agents synthesized in these conditions, which is a prerequisite to minimize the formation of free polymer particles during emulsion polymerization reactions carried out in the presence of these RAFT copolymers adsorbed at the surface of inorganic particles. Indeed, the fact that block copolymers would be less efficient than the corresponding random or gradient copolymers was initially mentioned by Nguyen et al.[1] in their first article describing the synthesis of hybrid latexes via the macro-RAFT strategy. In addition, in the recent study reported by Zgheib et al.[2], the authors attempted to achieve the polymer encapsulation of cerium oxide nanoparticles in the presence of a PAA RAFT homopolymer, expecting that the in situ formation of PAA-*b*-poly(BA-*co*-

MMA) block copolymers would lead to the formation of CeO_2/polymer hybrid particles: the fact that this strategy only led to the formation of cerium oxide-free latex particles strongly suggests that block copolymers are less efficient than random or gradient copolymers for the synthesis of CeO_2-based hybrid latexes.

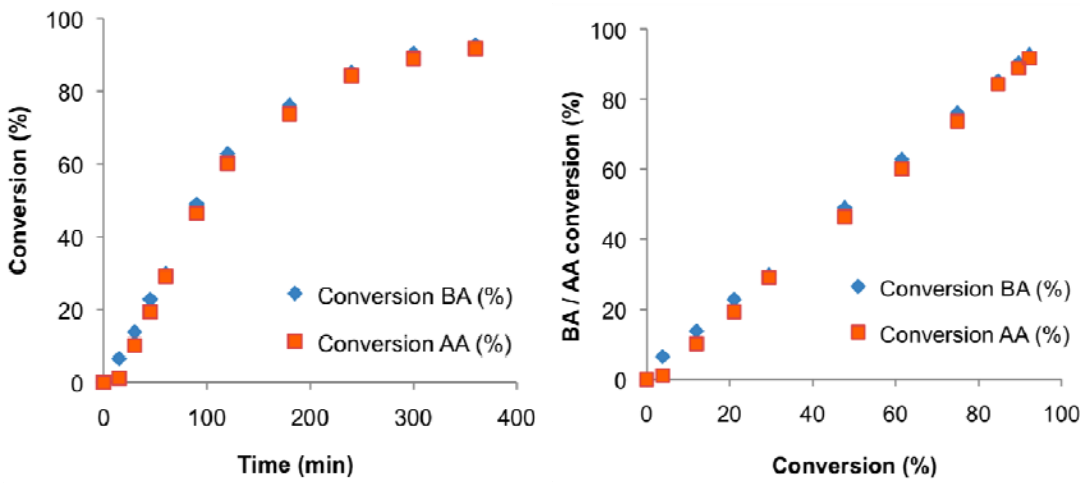

Figure SI.2. Butyl acrylate and acrylic acid conversions as a function of time (left) and as a function of the total monomer conversion (right).

1.2.3. Matrix Assisted Laser Desorption Ionization - Time of Flight – Mass Spectrometry (MALDI-ToF-MS)

MALDI-ToF-MS analyses were performed on a PerSeptive Biosystems Voyager-DE Biospectrometry Workstation to verify the chain-end functionality of the copolymer (Figure SI.3). Poly(BA-*co*-AA) oligomer samples were prepared as follows: a 40 mg/mL trans-2-[3-(4-tertbutylphenyl)-2-methyl-2-propenylidene] (DCTB) matrix sample and a 5mg/mL potassium trifluoroacetate sample were prepared in tetrahydrofuran. A 1 mg/mL oligomer solution was prepared in THF and mixed with the matrix and cationization agent solutions in a 4:4:1 volume ratio (oligomer : matrix : potassium trifluoroacetate). A 3 µL drop was

deposited and dried on a V700666 sample plate SS (Applied Biosystems). Analyses were carried out in positive reflector mode, with a total of 1000 shots per measurement.

As expected, the interval between peaks of a same series are equal to the isotopic masses of the two monomers (M_{BA} = 128.08 g/mol and M_{AA} = 72.02 g/mol). The main series (**a**) was attributed to the structure of the macro-RAFT agent associated with a potassium cation, while the structure corresponding to the series **c** was assumed to be formed by fragmentation of the trithiocarbonate function (Table SI.3). We assume that series **b** corresponded to the formation of a disulfide bond by air oxidation of the complementary thiol structures. This is in agreement with results reported by Llauro et al.[3] who characterized different types of chain ends encountered in poly(acrylic acid) RAFT homopolymers. They established that the proportion of such secondary structures was less than 12% in the whole homopolymer. Despite a small shift compared to m/z values calculated for these structures, experimental m/z values are in good agreement with theoretical values. From this analysis we may thus conclude that poly(BA-*co*-AA) RAFT copolymers display the main expected functionality: two benzyl groups on each chain end and a trithiocarbonate function at a random position inside the polymer chain.

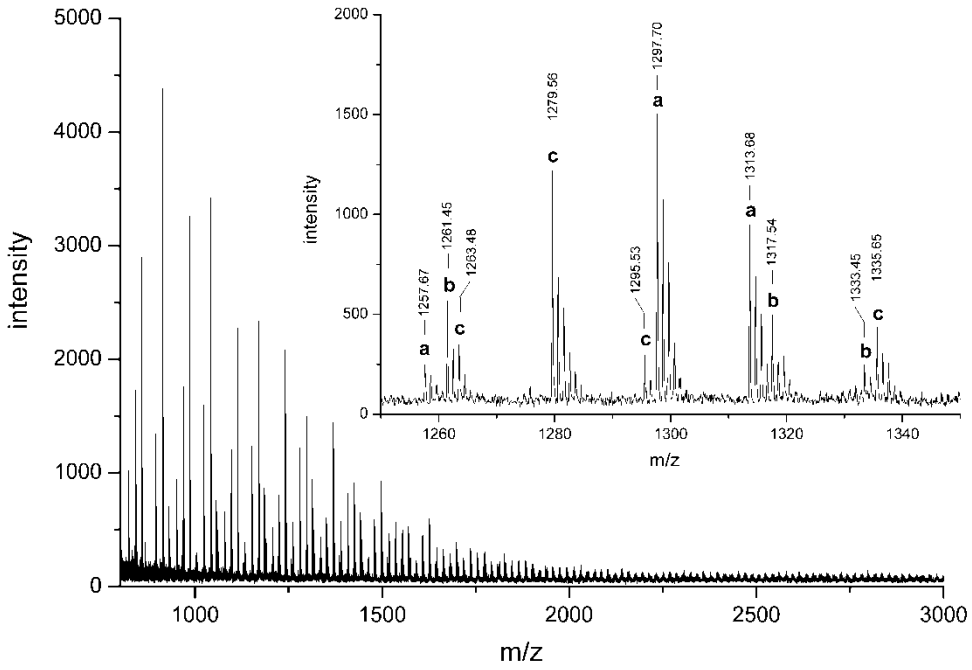

Figure SI.3. MALDI-ToF-MS spectrum of the RAFT copolymer with a BA_5-*co*-AA_5 targeted composition.

Table SI.3. Assignment of the peaks in the enlarged region of the MALDI-ToF-MS spectrum of the RAFT copolymer with a BA_5-*co*-AA_5 targeted composition.

Series and structure	x	y	m/z theo	m/z exp
a 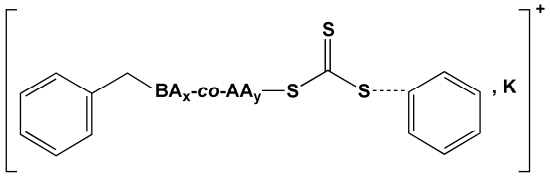	5	4	1257.49	1257.67
	7	1	1297.60	1297.70
	6	3	1313.56	1313.68
b 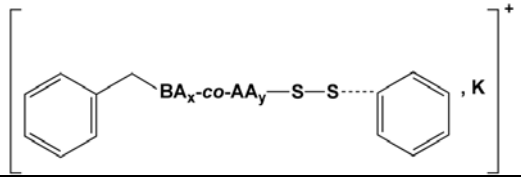	2	10	1261.40	1261.45
	3	9	1317.46	1317.54
	2	11	1333.42	1333.45
c	6	4	1263.56	1263.48
	5	6	1279.52	1279.56
	4	8	1295.47	1295.53

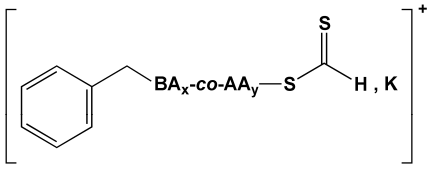	6	4	1335.58	1335.65

2. ^{1}H NMR kinetic analyses of the RAFT copolymerization of butyl acrylate and AMPS

To follow the conversions of both monomers (butyl acrylate and AMPS) against time, a time-dependent ^{1}H NMR analysis was performed in parallel of reaction A2', on a 0.6 mL sample of the reaction medium placed in a NMR tube with 3 capillaries containing deuterated benzene C_6D_6 and analyzed for 10 hours at 70°C in a 250 MHz Bruker NMR spectrometer. Monomer conversions were determined following a similar procedure to the one employed previously in the case of butyl acrylate and acrylic acid: integration peak **a** corresponding to aromatic protons of benzyl chain ends was taken as an internal standard and the integrations of peaks **b** and **c** (integrating for specific protons of butyl acrylate and AMPS respectively) (Figure SI.4) were used to calculate the conversions of the two monomers as a function of time:

$$X_{BA,\,t}\,(\%) = (b_{t=0} - b_t) \times 100 / b_{t=0} \qquad (4)$$

$$X_{AMPS,\,t}\,(\%) = (c_{t=0} - c_t) \times 100 / c_{t=0} \qquad (5)$$

where $X_{BA,\,t}$ and $X_{AMPS,t}$ are the conversions of butyl acrylate and AMPS respectively at time t, $b_{t=0}$, $c_{t=0}$ the integration values of peaks **b** and **c** at initial time and b_t and c_t are the integration values of peaks **b** and **c** at time t.

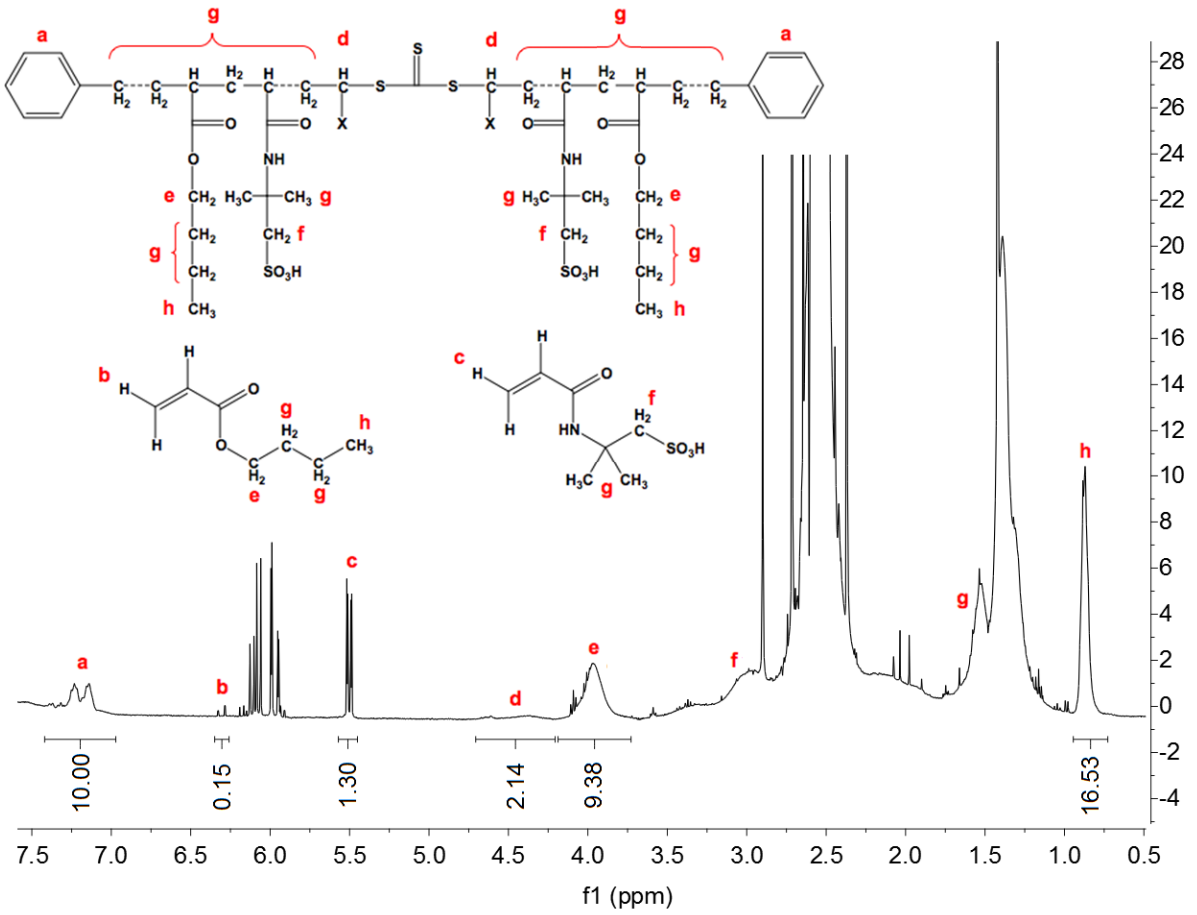

Figure SI.4. ^{1}H NMR spectrum and corresponding integration peaks of the poly(BA-*co*-AMPS) RAFT copolymer A2' with a BA_5-*co*-$AMPS_5$ targeted composition (crude reaction product diluted in DMSO-d_6).

3. Characterization of poly(BA-*co*-AMPS) and poly(BA-*co*-AA-*co*-AMPS) macro-RAFT agents by MALDI-ToF-MS

3.1.3. Experimental procedure

MALDI-ToF-MS analyses were performed on a PerSeptive Biosystems Voyager-DE Biospectrometry Workstation. Poly(BA-*co*-AMPS) and poly(BA-*co*-AA-*co*-AMPS) macro-RAFT agent samples were prepared as follows: a saturated solution of α-Cyano-4-hydroxycinnamic acid (HCCA) matrix was prepared in ethanol. A 1 mg/mL oligomer

solution was prepared in ethanol and mixed with the matrix solution in a 20:1 volume ratio (oligomer : matrix). A 3 µL drop was deposited and dried on a V700666 sample plate SS (Applied Biosystems). Analyses were carried out in linear negative mode, with a total of 1000 shots per measurement.

3.2.3. MALDI-ToF-MS characterization of poly(BA-co-AMPS) RAFT copolymers

MALDI-ToF-MS analyses were carried out in linear negative mode on the RAFT copolymer with a BA_5-*co*-$AMPS_5$ targeted composition (Figure SI.5).

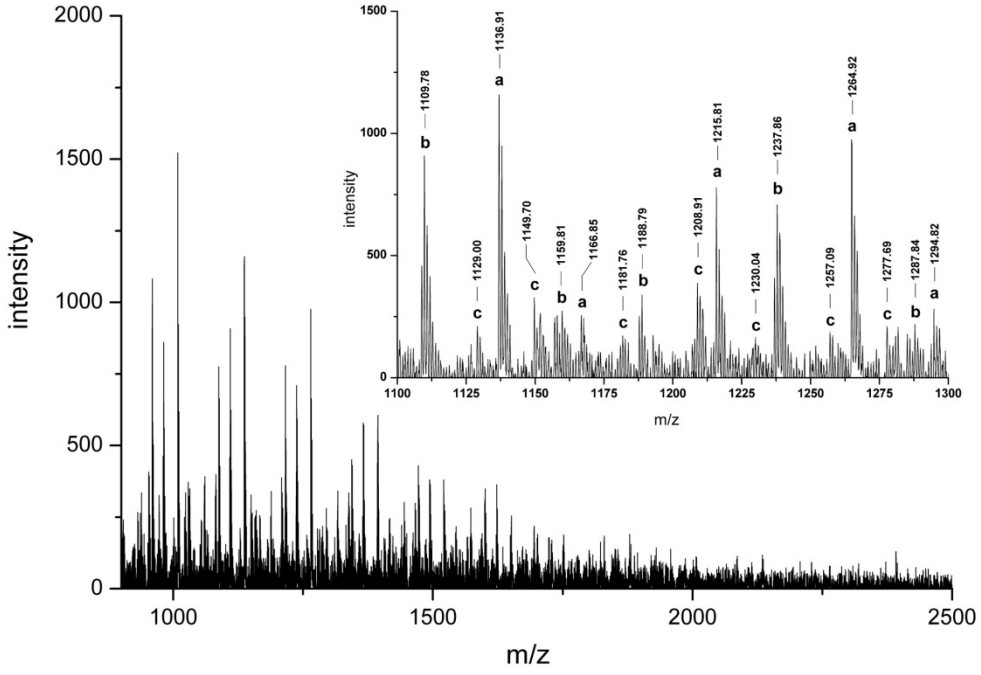

Figure SI.5. MALDI-ToF-MS spectrum of the RAFT copolymer with a BA_5-*co*-$AMPS_5$ targeted composition.

Peaks corresponding to the main series (**a**) were attributed to the expected macro-RAFT agent structure, with two benzyl groups as chain ends and a trithiocarbonate function situated inside the polymer chains. A second structure (series **b**) was identified as carrying a

sulfine end-group that may originate from the fragmentation and oxidation of the trithiocarbonate group[4] occurring during the analysis. For both series **a** and **b**, an acceptable agreement could be observed between theoretical and experimental m/z values (Table SI.4). A third structure (**c** series) was assumed to correspond to the thiol-ended polymer chains, also formed by fragmentation of the trithiocarbonate function during the analysis and complementary to structure **b**. However, comparison of theoretical isotopic masses to experimental data tends to question this assumption. Yet it is reasonable to assume that the extensive noise observed in this spectrum may have complicated the attribution of the main isotopic peaks corresponding to the **c** series.

Table SI.4. Assignment of the peaks in the enlarged region of the MALDI-ToF-MS spectrum of the RAFT copolymer with a BA_5-*co*-$AMPS_5$ targeted composition.

Series and structure	x	y	m/z theo	m/z exp
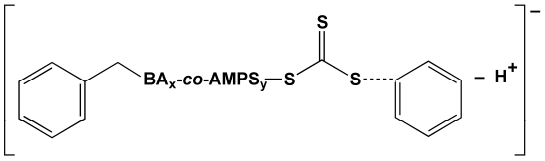 **a**	5	1	1136.49	1136.91
	2	3	1166.36	1166.85
	4	2	1215.47	1215.81
	6	1	1264.58	1264.92
	3	3	1294.44	1294.82
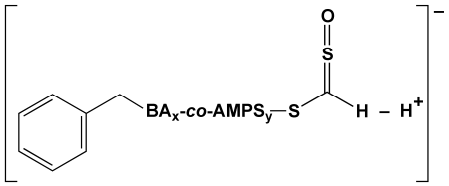 **b**	4	2	1109.44	1109.78
	6	1	1158.55	1159.81
	3	3	1188.42	1188.79
	5	2	1237.53	1237.86
	7	1	1286.64	1287.84
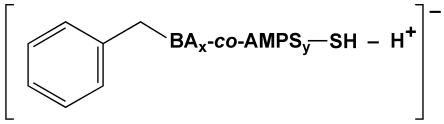	3	3	1128.45	1129.00
	8	0	1147.70	1149.70
	5	2	1177.56	1181.76

c	2	4	1207.42	1208.91
	7	1	1226.67	1230.04
	4	3	1256.53	1257.09
	9	0	1275.78	1277.69

3.2.3. MALDI-ToF-MS characterization of poly(BA-co-AA-co-AMPS) RAFT terpolymers

MALDI-ToF-MS analyses, measured in linear negative mode on the terpolymer with a BA_5-*co*-AA_5-*co*-$AMPS_4$ targeted composition were more difficult to interpret due to the multitude of possible structures obtained from different combinations of the three comonomers (Figure SI.6). The main series (**a**), corresponding to the sulfine-ended polymer chain, was still attributed to the fragmentation and oxidation of the trithiocarbonate function occurring during the analysis (Table SI.5).

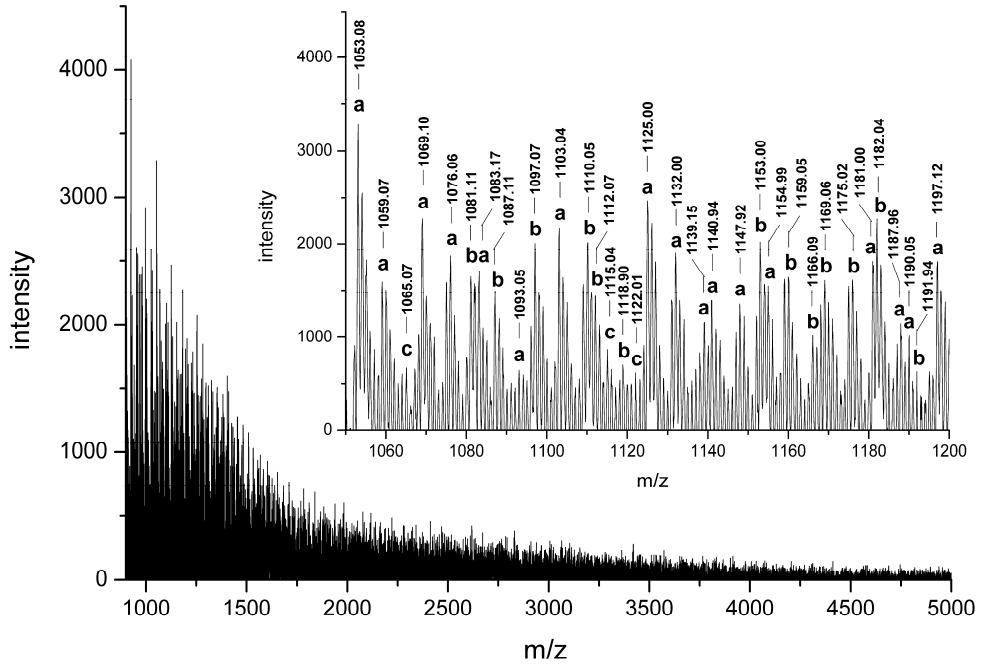

Figure SI.6. MALDI-ToF-MS spectrum of the RAFT terpolymer with a BA_5-*co*-AA_5-*co*-$AMPS_4$ targeted composition.

Series **b** was assigned to the expected RAFT terpolymer structure with two benzyl end groups and a trithiocarbonate function situated inside the polymer chain. A third series (**c**), still attributed to the thiol-ended fragment, was hardly visible in the spectrum due to overlapping of the isotopic peaks from the two other series.

Table SI.5. Assignment of the peaks in the region 1100 < m/z < 1150 of the MALDI-ToF-MS spectrum of the RAFT terpolymer with a BA_5-*co*-AA_5-*co*-$AMPS_4$ targeted composition.

Series and structure	x	y	z	m/z theo	m/z exp
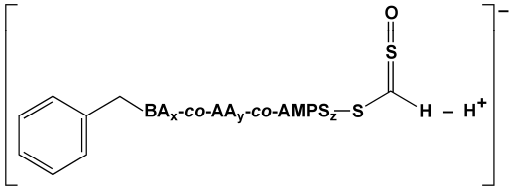 **a**	5	1	1	1102.49	1103.04
	3	2	2	1125.40	1125.00
	2	1	3	1132.35	1132.00
	1	0	4	1139.30	1139.15
	2	4	2	1141.36	1140.94
	1	3	3	1148.31	1147.92
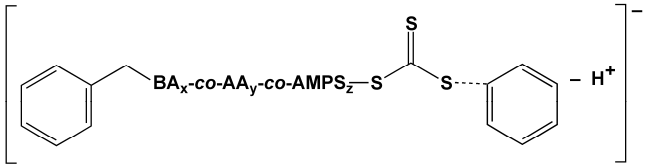 **b**	1	1	3	1110.29	1110.05
	2	5	1	1112.35	1112.07
	1	4	2	1119.30	1118.90
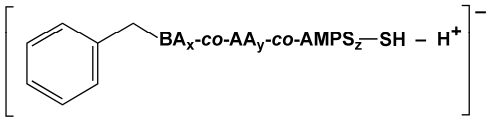 **c**	5	2	1	1114.54	1115.04
	4	1	2	1121.50	1122.01

4. Characterization of the adsorption of amphiphatic macro-RAFT agents by UV-visible spectrometry

The following example is given in the case of the RAFT terpolymer with a BA_5-*co*-AA_5-*co*-$AMPS_4$ targeted composition. For each type of amphiphatic macro-RAFT agents, a

calibration curve, giving the maximum absorbance (at 308 nm, specific for the trithiocarbonate function) as a function of the oligomer concentration in water (from 0.005 to 0.3 g/L), was plotted (Figure SI.7). The calibration curves followed a linear trend for values of absorbance below 2.

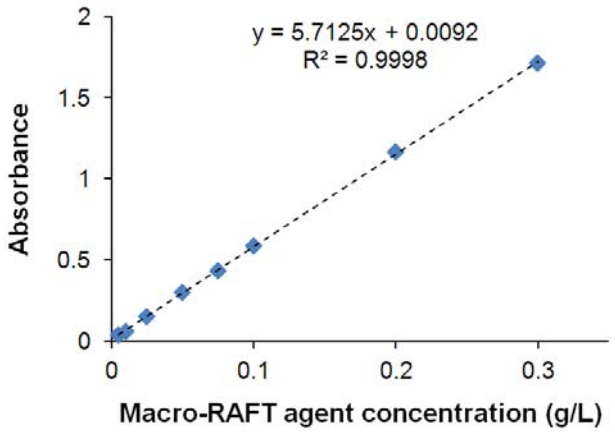

Figure SI.7. Calibration curve obtained with the RAFT terpolymer with a BA_5-*co*-AA_5-*co*-$AMPS_4$ targeted composition.

Serum solutions, containing the portion of macro-RAFT present in the aqueous phase, obtained after ultracentrifugation of cerium oxide dispersions, were analyzed by UV-visible spectroscopy (Figure SI.8). Dilutions of 10 or 100 times were required in order to fit the linear range of absorbance of the calibration curve. From the maximum absorbance measured at 308 nm for each solution, the concentration of macro-RAFT agent could be determined via the calibration curve (Table SI.6). A test sample (A2''-T), obtained by dilution of an ultracentrifugated solution of the RAFT terpolymer in water in the absence of cerium oxide, was also analyzed to verify the precision of the measurement.

The mass of macro-RAFT agent adsorbed per gram of cerium oxide ($m_{macro\text{-}RAFT\ /\ g\ CeO2}$) could then be calculated via a mass balance equation:

$$m_{\text{macro-RAFT / g CeO2}} = ([\text{macro-RAFT}]_0 - [\text{macro-RAFT}]_{\text{serum}}) / [CeO_2]_0 \quad (6)$$

where $[\text{macro-RAFT}]_0$ and $[CeO_2]_0$ (expressed in g/L) correspond respectively to the macro-RAFT agent concentration and the cerium oxide concentration in the initial CeO_2 dispersion (before ultracentrifugation), and $[\text{macro-RAFT}]_{\text{serum}}$ is the macro-RAFT agent concentration in the serum (in g/L).

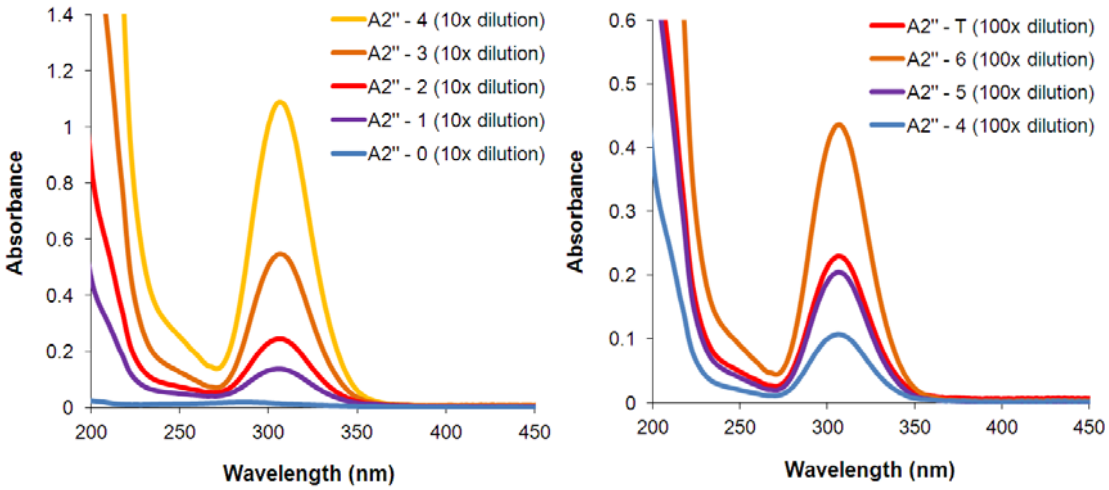

Figure SI.8. UV-visible absorption curves of serum solutions obtained after ultracentrifugation of cerium oxide dispersions.

Table SI.6. Characterization of the adsorption of the RAFT terpolymer with a BA_5-*co*-AA_5-*co*-$AMPS_4$ targeted composition at the surface of CeO_2 nanoparticles via UV-visible spectroscopy.

	Initial CeO_2 dispersion		**Characterization of serum solutions**			
Entry	**CeO_2 concentration (g/L)**	**Macro-RAFT concentration (g/L)**	**Dilution**	**Absorbance**	**Macro-RAFT concentration in serum (g/L)**	**Mass of macro-RAFT per gram of CeO_2 (g/g)**

A2''-0	4.0	0	10 x	0.013	/	/
A2''-1	4.0	0.2	10 x	0.136	0.23	0.00
A2''-2	4.0	0.4	10 x	0.244	0.42	0.00
A2''-3	4.0	1.0	10 x	0.546	0.95	0.01
A2''-4	4.0	2.0	10 x	1.090	1.90	0.03
A2''-5	4.0	4.0	100 x	0.205	3.75	0.06
A2''-6	4.0	8.0	100 x	0.436	7.80	0.05
A2''-T	0	4.0	100 x	0.229	4.17	n.a.

References

[1] D. Nguyen, H. S. Zondanos, J. M. Farrugia, A. K. Serelis, C. H. Such, B. S. Hawkett, Langmuir 24 (2008) 2140.

[2] N. Zgheib, J.-L. Putaux, A. Thill, E. Bourgeat-Lami, F. D'Agosto, M. Lansalot, Polym. Chem. 4 (2013) 607.

[3] M.-F. Llauro, J. Loiseau, F. Boisson, F. Delolme, C. Ladaviere, J. Claverie, J. Polym. Sci., Part A : Polym. Chem. 42 (2004) 5439.

[4] A. Favier, C. Ladaviere, M.-T. Charreyre, C. Pichot, Macromolecules 37 (2004) 2006.